RSC Advances

ROYAL SOCIETY OF CHEMISTRY

www.rsc.org/advances

Cu-Ag/Hydrotalcite Catalysts for Dehydrogenative Cross-Coupling of Primary and Secondary Benzylic Alcohols

Jin Xu [a,b], Hongmei Yue [a,b], Sheng Liu [a,b], Hanfei Wang [a,b], Yuqun Du [a,b], Chunli Xu [a,b,*], Wensheng Dong [a,b], Chunling Liu [a,b]

[a] Key Laboratory of Applied Surface and Colloid Chemistry (Shaanxi Normal University), Ministry of Education, Xi'an 710119, PR China

[b] School of Chemistry and Chemical Engineering, Shaanxi Normal University, Chang'an West Street 620, Xi'an 710119, PR China

* Corresponding author.

School of Chemistry and Chemical Engineering, Shaanxi Normal University, 620 Chang'an West Street, Xi'an 710119, PR China

Tel: 86-29-81530779

E-mail: xuchunli@snnu.edu.cn

Abstract

The development of new and inexpensive heterogeneous catalysts for direct C-C cross-coupling of primary and secondary alcohols is a challenging goal and has great importance in academic and industrial sectors. In this work Cu-Ag/hydrotalcite (Cu-Ag/HT) catalysts were prepared and tested for their impact on this cross-coupling. Effect of supports, including MgO, γ-Al_2O_3 and HT with different Mg:Al molar ratios, was investigated. It was found that the acidic or basic properties of the supports affected product selectivity. The roles of Cu and Ag sites in the cross-coupling were also investigated with the prepared Cu-Ag/HT catalyst demonstrating high activity and selectivity for the reaction. The yield-to-target product of β-phenylpropiophenone reached 99% after 1 h under optimum reaction conditions. Stability in air and reusability studies finds that Cu-Ag/HT can be stored for 6 days and can be used five times without apparent deactivation, respectively.

Keywords: Cu-Ag nanoparticles, Hydrotalcite, Alcohol cross-coupling, Acceptorless dehydrogenation.

1. Introduction

Acceptorless dehydrogenation reactions, in which hydrogen is liberated and new prospective bonds are generated by further reactions of the dehydrogenated products, are emerging as an atom-economical and environmentally benign synthetic method, circumventing the need for

stoichiometric oxidants or the prefunctionalization of substrates [1,2]. The self-coupling of an alcohol or the cross-coupling of two different alcohols constitutes a key transformation in reaction schemes targeting higher yields of alcohols, ketones, and esters [3]. The homodimerization of primary and secondary alcohols, the so-called Guerbet reaction, has been known for more than a century [3,4]. However, the reaction has recently been extended to the cross-coupling (selective *β*-alkylation) of secondary alcohols with primary alcohols (Scheme 1) [5].

Several reports have demonstrated the *β*-alkylation of secondary alcohols with primary alcohols under the catalysis of Ru and Ir complexes [5-8]. However, a number of limitations exist for these processes. These limitations include low catalytic turnover numbers, the requirement of a large amount of a strong base, and expensive catalysts, which are also difficult to synthesize and unable to be reused [9]. These limitations reinforce the need for a ligand-free, reusable catalyst system for this type of transformation. To date, there are three related examples of heterogeneous catalysis [9-11]. Ag/Al_2O_3 [9] and Pd/C [10] have been used as efficient catalysts for direct C-C cross-coupling of secondary and primary alcohols. However, a sacrificial hydrogen acceptor and/or a considerable amount of inorganic homogeneous base was required to achieve a high selectivity. Au-Pd/hydrotalcite (Au-Pd/HT) catalysts have been shown to avoid the need for a hydrogen acceptor and homogeneous

base as well as exhibiting high catalytic performance [11]. However, Au and Pd are precious metals with relatively scarce global reserves. The development of new and inexpensive heterogeneous catalysts for the reaction is therefore a challenging goal and has great importance in academic and industrial sectors [12].

The reaction proceeds by dehydrogenation of the alcohol to an intermediate carbonyl compound. This is followed by an Aldol condensation with the ketone to yield an α,β-unsaturated carbonyl derivative, which is finally reduced by the metal hydride to give the corresponding carbonyl compound (Scheme 2) [9]. A key concept in the catalyst design in some of the systems is the multifunctionality of metal-loaded acidic and/or basic metal oxides. Here, the acidic and/or basic sites selectively catalyze the Aldol condensation reactions while the metal sites catalyze the transfer dehydrogenation of alcohol and transfer hydrogenation of the condensation products as intermediates [5,13]. Catalysts based on Cu have attracted much attention in heterogeneous catalysis because of the metal's relative cost advantage [14-16]. Such catalysts have been reported to provide high activity in the dehydrogenation of alcohols and hydrogen transfer [17,18]. The catalytic performance of Cu was reportedly affected by the coexistence of Ag nanoparticles [19,20]. HT showed high activity for the Aldol condensation [11,21]. Therefore, Cu-Ag/HT may offer the potential for

catalyzing the reaction, the investigation of which is the focus of this work.

2. Experimental section

2.1 Catalyst preparation

2.1.1 Preparation of supports

The HT support was prepared using a standard aqueous co-precipitation method, which we have described previously [22]. An aqueous solution (160 mL) of metal nitrates in different Mg^{2+}:Al^{3+} molar ratios with a total concentration of 1.5 M was mixed slowly by continuous stirring with an alkaline solution of Na_2CO_3-NaOH. The molar ratio of Na_2CO_3 to Al^{3+} was 2:1. The pH of the mixture was maintained between a value of 9 and 10 by adjusting the flow rate of the alkaline solution. The temperature was maintained at 25 °C. Following this addition, which resulted in the formation of heavy slurry, the mixture was aged at 60 °C for 18 h by stirring to selectively facilitate the growth of the precipitated HT phase. The slurry was then cooled to 25 °C, filtered, and washed with water until the pH value of the filtrate was approximately 7. The precipitate was dried at 110 °C for 12 h. Depending on the initial conditions, the resulting material was HT with a Mg^{2+}:Al^{3+} molar ratio of 1:1, 2:1, 3:1, or 5:1. Hereafter, unless noted otherwise, HT describes a 2:1 molar ratio of Mg^{2+}:Al^{3+}.

A mesoporous MgO support for the Cu-Ag catalyst was prepared by

calcining commercially available $Mg(OH)_2$ (99%, Guangdong Shantou Hongwei Chemical Plant, P.R. China) at 500 °C for 3 h in static air (muffle oven, heating rate: 10 °C min^{-1}). A γ-Al_2O_3 support was prepared by calcining a commercial sample of γ-Al_2O_3 (Alfa Aesar) under the same conditions.

2.1.2 Synthesis of the Cu-Ag supported catalyst

Cu_xAg_{1-x}/HT (where $0 \leq x \leq 1$) catalysts were prepared by a co-impregnation method. A mixture of the support and an aqueous solution of Ag(I) and Cu(II) nitrates was stirred at 80 °C for 2 h, followed by drying at 120 °C for 12 h, calcination in air at 300 °C for 5 h, and reduction in H_2 at 300 °C for 2 h. $Cu_{0.95}Ag_{0.05}$/HT (x = 0.95) with a total metal (Cu + Ag) loading of 1 wt% was used as the standard catalyst. Using a similar method, Cu_xAg_{1-x}/γ-Al_2O_3 and Cu_xAg_{1-x}/MgO were also prepared.

2.2 Characterization of catalyst

The surface area and pore characteristics of the catalysts were determined using a Micromeritics ASAP 2020 instrument (USA). The sample was degassed at 110 °C for 6 h in N_2 prior to carrying out surface area measurements. Nitrogen adsorption and desorption isotherms were measured at −196 °C. The specific surface areas of the catalysts were determined by applying the Brunauer–Emmett–Teller (BET) method to the nitrogen adsorption data obtained in the relative pressure range of

0.06 to 0.30. The total pore volume of the samples was estimated from the amount of nitrogen adsorbed at a relative pressure of 0.995. Pore volume and pore size distributions were obtained from analysis of the desorption branches of the nitrogen isotherms using the Barrett–Joyner–Halenda method.

X-ray diffraction (XRD) patterns were recorded using a D/Max-3C X-ray powder diffractometer (Rigaku Co, Japan), with a Cu–K source fitted with an Inel CPS 120 hemispherical detector.

Scanning transmission electron microscopy (STEM) micrographs were obtained using a FEI Tecnai G2 F20 instrument (USA).

Elemental analysis of HT was carried out by an FEI Quanta 200 (USA) scanning electron microscope equipped with energy-dispersive X-ray spectroscopy.

The loading of Cu-Ag was determined by inductively coupled plasma mass spectrometry (Bruker, M90; Germany).

X-ray photoelectron spectroscopy (XPS) was used to characterize the valence of catalysts. XPS data was obtained in an Axis Ultra spectrometer (Kratos Analytical Ltd., Japan) using AlKα ($h\upsilon$ = 1486.6 eV) X-ray radiation at an energy of 150 W.

NH_3-temperature-programmed desorption (TPD) and CO_2-TPD were performed on a Micromeritics AutoChem 2920 II instrument. Typically, the sample loaded in a quartz reactor was pretreated with high-purity He

at 350 °C for 1 h. After cooling the sample to 100 °C, CO_2 adsorption was performed by switching the He flow to a CO_2-Ar (5 vol % CO_2) gas mixture and then maintaining the sample at 100 °C for 3 h. The gas-phase (and/or weakly adsorbed) CO_2, was purged by high-purity He at the same temperature. CO_2-TPD was then performed in the He flow by raising the temperature to 800 °C at a rate of 10 °C·min^{-1}. The desorbed CO_2 molecules were detected by using a MKS Cirrus 2 mass spectrometer. NH_3-TPD was performed by using a similar procedure.

2.3 Reaction procedure

The cross-coupling of primary and secondary alcohols was carried out using a 50 mL, three-necked, round-bottomed flask with a water-cooled condenser. Typically, the reactor was charged with 0.1 g of catalyst, 1.0 mmol of benzyl alcohol, 1.0 mmol of 1-phenylethanol, and 3 mL of *o*-xylene. This mixture was then heated at 150 °C for 1 h under N_2 at 1 atm. After cooling to room temperature, the resulting mixture was diluted to a constant volume with toluene in a 15 mL volumetric flask. The reaction products were quantitatively analyzed by a Shimadzu GC-2014 (Rtx®-5, 30 m × 0.32 mm × 0.25 μm) gas chromatograph equipped with a flame ionization detector. N-dodecane (1 mmol) was used as the internal standard for analysis. The products were identified by ^{1}H NMR as well as GC-MS.

3. Results and discussion

3.1 Catalyst characterization

3.1.1 BET surface area and pore size

As shown in Table 1 (Entries 2 to 5), the surface area of Cu-Ag/HT was approximately 200 $m^2 g^{-1}$, which was irrespective of the Mg:Al ratio (from 1:1 to 5:1). The surface area of Cu-Ag/γ-Al_2O_3 (Table 1, Entry 1) was similar to that of Cu-Ag/HT. Cu-Ag/MgO had the lowest surface area of 125 $m^2 g^{-1}$. The isotherms of the six samples exhibited the characteristic Type IV shape, which, together with the pore size distribution results, suggested that the samples were mesoporous materials.

3.1.2 XRD analysis

Figures 2–4 display the XRD patterns of the supports and Cu-Ag catalysts. Results for HT supports with 1:1 molar ratio of Mg:Al showed major diffraction peaks for HT and minor diffraction peaks for Al_2O_3 (Fig. 2a). For HT supports with molar ratios of 2:1, 3:1, and 5:1, the results were the same as those for HT, with characteristic diffraction peaks at 11.4, 23.0, and 34.9° (Fig. 2b–d) [22]. Cu-Ag/HT results showed the diffraction peaks characteristic of MgO, which were observed irrespective of the Mg:Al molar ratio and distinct from the corresponding peaks from their HT supports (Fig. 2e). In the XRD spectra of Cu-Ag/HT, a diffuse diffraction diagram of MgO only was observed, and Al_2O_3 formed a separate amorphous phase without diffraction pattern in XRD [23-25].

This indicated that the HT supports were transformed into mixed oxide in the process of preparing Cu-Ag/HT catalysts. Results for γ-Al_2O_3 and Cu-Ag/γ-Al_2O_3 were similar, showing the typical features of γ-Al_2O_3 (Fig. 3) [22]. This indicated that the crystalline structure of the γ-Al_2O_3 supports did not change after supporting the Cu-Ag phase. Results for MgO and Cu-Ag/MgO were also similar to each other. No reflections corresponding to Cu or Ag were observed for catalysts loaded with 1 wt% of catalyst because of the low loadings (Figs. 2 and 3). XRD patterns of 10 wt% Cu-Ag/HT were also determined (Fig. 4) and show reflections corresponding to Cu because of the increased catalyst loading.

3.1.3 XPS analysis

XPS results for 1 wt% Cu-Ag/HT did not clearly show the XPS spectra of Ag because of its low loading. Therefore, the total loading amount of Cu-Ag was increased to 10 wt%. XPS spectra of the Cu 2p and Ag 3d regions for 10 wt% Cu-Ag/HT are given in Fig. 5. All of the spectra of the Cu 2p region could be satisfactorily fitted with maximum peaks at binding energies of 932.9 and 953.1 eV, characteristic of metallic Cu. No $Cu^{\delta+}$ was detected, suggesting that Cu had been reduced completely. All of the spectra of the Ag 3d region could be satisfactorily fitted with maximum peaks at binding energies of 367.8 and 374.0 eV, characteristic of metallic Ag. This indicated that Ag had been reduced completely.

To study the resistance to oxidation of Cu-Ag bimetallic nanoparticles, XPS spectra of Cu-Ag/HT were taken after samples had been stored for 2 or 3 months (Fig. 6). Spectra of Cu 2p for Cu-Ag/HT samples that had been stored showed the characteristics of metallic Cu and were similar to the results from the fresh catalysts. In contrast, the XPS spectra of Cu 2p for Cu/HT samples that had been stored exhibited peaks associated with Cu^{2+} alongside the characteristic peaks of metallic Cu [20, 26]. This indicated that part of the Cu nanoparticles on Cu/HT had been oxidized to Cu^{2+} by air. This also suggested that the Cu atoms of the Cu-Ag bimetallic nanoparticles were less oxidized than those in the pure Cu nanoparticles. The enhanced resistance to oxidation of Cu-Ag bimetallic nanoparticles was ascribed to the addition of Ag [20]. The structure and resistance to oxidation of Cu-Ag bimetallic nanoparticles have been investigated in the literature [20,27-30]. The results from the literature about Cu-Ag nanoparticles indicated that Cu nanoparicles are easily oxidized, and the addition of Ag to Cu enhanced the resistance of Cu to oxidation. The enhanced resistance was ascribed to the smaller number of surface-exposed Cu atoms compared to the entire Cu atoms in this Ag-Cu bimetallic nanoparticles and electronic interaction between Ag and Cu atoms in the Ag-Cu bimetallic nanoparticles.

3.1.4 TEM analysis

The morphological and structural properties of Cu-Ag/HT were

further characterized by STEM, selected-area electron diffraction (SAED), and high-resolution TEM (HR-TEM), as shown in Fig. 7. The Cu-Ag nanoparticles that were calcined and reduced at 300 °C were too small to see in STEM images (Fig. $7a_1$) while for the process at 600 °C they were large enough to be easily observed (Fig. $7b_1$). The higher calcination temperature could have resulted in the observed increase in the size of the nanoparticles [31,32].

The SAED patterns indicated that the Cu-Ag nanoparticle was polycrystalline. Each ring of the SAED image is a reflection of planes with different interplanar spacings [20]. Using the length of scale (L) and the radius of the diffraction ring (R) in the equations L/5=R/N and X=1/N (where N is the reciprocal spacing and X is the spacing), X values of 2.47, 1.79, and 1.33 Å were obtained. The spacing values of nanoparticles in the samples were consistent with those of lattice planes (111), (200) and (220) of Cu nanoparticles. Combined with the XPS and XRD analysis, it can be concluded that both Cu and Ag nanoparticles were in a metallic state.

3.1.5 Acidity and basicity of supports

The acidity and basicity of the supports were determined by TPD, and the results are shown in Fig. 8. The CO_2-TPD profiles of HT supports shows two big desorption peaks at 138 °C and 520 °C, respectively, as well as two small desorption peaks at 288 °C and 662 °C, respectively.

MgO had two main desorption peaks at 158 °C and 562 °C, respectively. The CO_2-TPD profiles of γ-Al_2O_3 supports only shows one small desorption peaks at 138 °C. From the temperature and intensity of the CO_2 desorption peaks, it can be found that HT and MgO possessed relatively strong basicity, while γ-Al_2O_3 had weak basicity. The NH_3-TPD profiles of HT supports shows two big desorption peaks at 166 °C and 441 °C, respectively. γ-Al_2O_3 had one broad peak at 200 °C. In case of MgO, no desorption peak was observed. From the temperature and intensity of the NH_3 desorption peak, we can see that HT and γ-Al_2O_3 possessed relatively strong acidity, while MgO had no significant acidity.

3.2 Effect of supports

Analysis of γ-Al_2O_3, HT with different Mg^{2+}:Al^{3+} molar ratios, and MgO supports (Fig. 9) revealed that the supports affected both the activity and selectivity of Cu-Ag catalysts. When γ-Al_2O_3 was used as support, the conversion of benzyl alcohol was 75% (Fig. 9a). In the case of HT supports, the conversion of benzyl alcohol varied with the Mg^{2+}:Al^{3+} molar ratio. At a molar ratio of 1:1 the conversion was 50%, but this increased to a maximum of 88% when the molar ratio was 2:1. Above 2:1, the conversion decreased as Mg^{2+}:Al^{3+} was increased. When pure MgO was used as the support the conversion of benzyl alcohol was 64%.

The reaction produced two types of products (Scheme 3). Ether was

formed from the direct etherification of primary and secondary benzylic alcohols. Alternatively, β-phenylpropiophenone was formed by dehydrogenative cross-coupling of primary and secondary benzylic alcohols. When γ-Al_2O_3 was used as the support, ethers were produced (Fig. 9b). In contrast, when HT or MgO were the support only β-phenylpropiophenone was found. Furthermore, the yield of β-phenylpropiophenone varied with ratio of Mg^{2+}:Al^{3+}; at 1:1 the yield was 21%, but this increased to the maximum of 76% at 2:1. Above 2:1, the yield decreased as Mg^{2+}:Al^{3+} was increased. When pure MgO was used as the support, the yield of β-phenylpropiophenone decreased to 35%. Notably, *α,β,*-unsaturated carbonyl derivatives, for example, the intermediate 1,3-diphenyl-acrylketone, were not observed in the presence of Cu-Ag/HT or Cu-Ag/MgO.

The effect of the supports on the reaction selectivity was ascribed to whether the supports were acidic or basic. Acidic sites promoted the etherification of primary and secondary benzylic alcohols [33]. Conversely, strongly basic sites catalyzed the Aldol condensation step in the dehydrogenative cross-coupling of primary and secondary benzylic alcohols [5,13]. γ-Al_2O_3 includes weakly acidic sites [34], while HT and MgO have strong basic sites [35]. This explains why the main product was ether for Cu-Ag/γ-Al_2O_3, and β-phenylpropiophenone for Cu-Ag/HT and Cu-Ag/MgO.

The activity of pure, undoped γ-Al_2O_3 was also tested for the reaction between primary and secondary benzylic alcohols (Table 2). Here, as with Cu-Ag/γ-Al_2O_3, the products were also ethers, indicating that either Cu or Ag failed to function with the γ-Al_2O_3 support.

3.3 Effect of Cu:Ag mass ratio

Figure 10 shows that the conversion of benzyl alcohol and yield of β-phenylpropiophenone were lowest for the reaction using pure Ag, the latter being almost zero. Increasing the Cu content increased both the conversion and the yield with respective maximums of 88 and 76% observed after 0.5 h when the content of Cu was 95%. Using pure Cu caused the conversion and yield after 0.5 h to fall to 68% and 53%, respectively. These results suggested that the main active site was Cu, but that its activity was promoted by the presence of Ag. As shown in Fig. 6, the addition of Ag enhanced the resistance to oxidation of Cu. The role of Ag in the activity of Cu-Ag may be related to the increase in the resistance to oxidation of Cu. Besides, the presence of Ag may change the electronic and morphological structure of Cu, which affected the activity of Cu. The role of Ag will be studied in the future work.

3.4 Catalytic performance

The effect of calcination temperature and reaction conditions was studied (Figures S1-S3, and Tables S1 and S2). The results indicated that the optimum reaction conditions involved using 0.1 g of catalyst in a

reaction at a temperature of 150 °C that lasted 1 h. Under these conditions both the conversion of benzyl alcohol and the yield of β-phenylpropiophenone approached 99%.

Liu et al. [11] reported that Au-Pd/HT catalysts showed high catalytic performance for the reaction studied here. Indeed, they reported that both conversion and yield neared 97% after 5 h for a reaction involving primary alcohol (1 mmol), secondary alcohol (1 mmol), *p*-xylene (3 mL), and the Au-Pd/HT catalyst (0.38 g) in a N_2 atmosphere at 120 °C and 1 bar. Results for similar reaction conditions using Cu-Ag/HT catalyst showed that both the conversion of benzyl alcohol and the yield of β-phenylpropiophenone were similar to those obtained with Au-Pd/HT. Therefore, and given that Cu and Ag are more widely available and less expensive than Au and Pd, we suggest that Cu-Ag/HT is a better choice of catalyst for the dehydrogenation cross-coupling reaction of primary and secondary alcohols.

3.5 Coupling with various alcohols

With suitable reaction conditions established, the scope of substrates was then investigated (Table 3). Very high yields (90–100%) of the corresponding cross-coupled products were obtained from 1-phenylethanol and various substituted benzyl alcohols, including both electron-rich and electron-deficient examples (Table 3, Entries 1–5). Notably, electron-donating substituents on the primary alcohol appeared

to play a significant role, shortening the reaction time required to achieve completion (Entries 1–2). Conversely, *m*-substituted alcohols appeared to exhibit lower reaction rates and yields than *p*-substituted alcohols, likely because of steric effects (Entries 3–4). Similarly, excellent yields (97–99%) of the corresponding cross-coupled products were also obtained when using various substituted 1-phenyl-ethanol and benzyl alcohols, again including both electron–rich and electron-deficient examples (Entries 6–7).

The results also suggest that aliphatic primary alcohols are not suitable coupling partners. For example, when 2-phenylethanol was employed as the substrate, complete conversion and complete yield were obtained after 8 h (Entry 8). However, when cinnamyl primary alcohol was used as the substrate, the corresponding yield decreased to 58% after the same reaction period (Entry 9). Unfortunately, after 8 h none of the desired cross-coupled product was detected if aliphatic primary alcohols without benzene substituents, such as allyl alcohol or propyl alcohol, were employed as substrates (Entries 10–11). Instead these cases produced 1,3-diphenyl-1-butanone, which resulted from the self-coupling of 1-phenylethanol.

For the reactions of Entries 10–11 (Table 3), allyl alcohol or propyl alcohol kept unchanged when 1-phenylethanol occurred the dehydrogenative self-coupling. In the absences of allyl alcohol or propyl

alcohol, 1-phenylethanol still occurred the dehydrogenative self-coupling in similar yield. It was found that the cross-coupling and self-coupling competed with each other in the primary and secondary mixed alcohol system. As shown in Scheme 2, the first step of the reaction proceeds by dehydrogenation of the alcohol to an intermediate carbonyl compound. The dehydrogenation of aliphatic primary alcohols may go slowly in the presence of Cu-Ag/HT catalysts [36,37], whereas the rate of dehydrogenation of 1-phenylethanol was high. The low rate in dehydrogenation of aliphatic primary alcohols decreased the rate of cross-coupling between aliphatic primary alcohol and 1-phenylethanol, but did not affect the dehydrogenative self-coupling of 1-phenylethanol. This explained the reactions of Entries 10–11. However, for reactions of Entries 1–9, the detected products were mainly from the cross-coupling of primary and secondary alcohol, but not the self-coupling of alcohol. Furthermore, the yield to self-coupling of alcohol was very low and negligible. The high yield to cross-coupling of primary and secondary alcohol in Entries 1-9 was mainly ascribed to the property of the involved primary alcohol, which was various substituted benzyl alcohols. The various substituted benzyl alcohols was easily dehydrogenated to form the corresponding aldehyde [36,37], accordingly, easily cross-coupled with the secondary alcohol.

3.6 Stability in air and reusability of catalysts

3.6.1 Stability in air

Fresh Cu-Ag/HT and Cu/HT catalysts were stored in a desiccator for a number of days with their activity then tested to investigate the stability in air of Cu-Ag/HT. As shown in Fig. 11, the yield of β-phenylpropiophenone did not appear to change for catalysts stored for up to 6 days. However, after 9 days the yield decreased by 4% and fell by 18% after a total of 76 days. Cu/HT catalysts showed a faster decrease in yield than that of Cu-Ag/HT catalysts with the yield from reactions involving Cu/HT falling by 10 and 31% for 9 and 76 days, respectively. XPS analysis indicated that it was the addition of Ag, which enhanced the resistance to oxidation of Cu-Ag bimetallic nanoparticles, and was responsible for the extra longevity.

3.6.2 Reusability

Cu-Ag/HT catalysts were found to be usable five times with no apparent loss of activity (Table 4) with activity then declining to zero after the catalyst was used more than nine times. The deactivation of Cu-Ag/HT may be ascribed to structural change, especially the leaching of active sites of Cu and basic sites of Mg^{2+}. Indeed, the 0.95% loading of Cu in fresh catalyst decreased to 0.5% after it had been used nine times. Similarly, the molar ratio of Mg^{2+} to Al^{3+} in fresh Cu-Ag/HT was 2:1, but this decreased to almost 1.2:1 after nine uses. The decrease in loading amount of Cu and Mg^{2+}:Al^{3+} molar ratio showed that both Cu and Mg^{2+}

could leach into the reaction system. Further work will therefore focus on the prevention of the observed leaching of Cu and Mg^{2+} into the reaction system.

4 Conclusions

Acidic/basic properties of catalyst supports affected the activity and selectivity of Cu-Ag/HT in the reactions studied here. Acidic supports promoted the etherification of primary and secondary benzylic alcohols, whereas basic supports advanced the dehydrogenative cross-coupling of primary and secondary benzylic alcohols. Cu-Ag/HT with a 2:1 molar ratio of Mg to Al showed the highest activity and demonstrated it to be an active catalyst for the C-C cross-coupling of secondary and primary alcohols. The active sites of Cu-Ag/HT were Cu, with Ag involved in promoting the activity of Cu sites as well as hindering their oxidation. The yield of β-phenylpropiophenone reached 99% after 1 h under optimum reaction conditions. The catalyst also displayed reusability, with no loss of activity after five cycles, and resistance to oxidation, being able to be stored for 6 days without deactivation. However, the Cu-Ag/HT catalyst was completely deactivated after more than nine uses because of leaching of Cu and Mg^{2+} into the reaction system.

Acknowledgments

This work was supported by projects funded by the Natural Science Basic Research Plan in Shaanxi Province of China (Program No.

2013JM2003) and by the Fundamental Research Funds for the Central Universities (Program No. GK201505002).

References

[1] C. Gunanathan and D. Milstein, *Science*, 2013, **341**, 1229712.

[2] X. Liu, L. He, Y. Liu and Y. Cao, *Acc. Chem. Res.*, 2014, **47**, 793.

[3] I.S. Makarov and R. Madsen, *J. Org. Chem.*, 2013, **78**, 6593.

[4] J.T. Kozlowski and R.J. Davis, *ACS Catal.*, 2013, **3**, 1588.

[5] K. Shimizu, *Catal. Sci. Technol.*, 2015, **5**, 1412.

[6] S. Musa, L. Ackermann and D. Gelman, *Adv. Synth. Catal.*, 2013, **355**, 3077.

[7] D. Gnanamgari, C.H. Leung, N.D. Schley, S.T. Hilton and R.H. Crabtree, *Org. Biomol. Chem.*, 2008, **6**, 4442.

[8] D. Wang, K. Zhao, X. Yu, H. Miao and Y. Ding, *RSC Adv.*, 2014, **4**, 42924.

[9] K. Shimizu, R. Sato and A. Satsuma, *Angew. Chem.*, 2009, **121**, 4042.

[10] C.S. Cho, W.X. Ren and S.C. Shim, *Bull. Korean Chem. Soc.*, 2005, **26**, 1611.

[11] X. Liu, R. Ding, L. He, Y. Liu, Y. Cao, H. He and K. Fan, *ChemSusChem*, 2013, **6**, 604.

[12] L. Zhang, A. Wang , W. Wang ,Y. Huang , X. Liu, S. Miao , J. Liu and T. Zhang, *ACS Catal.*, 2015, **5**, 6563.

[13] J.D. Lewis, S.V. Vyver and Y. Román-Leshkov, *Angew. Chem. Int.*

Ed., 2015, **54**, 9835.

[14] P. Fakhri, B. Jaleh and M. Nasrollahzadeh, *J. Mol. Catal. A: Chem.*, 2014, **383– 384**, 17.

[15] G. Corro, S. Cebada, U. Pal, J.L.G. Fierro and J. Alvarado, *Appl. Catal. B*, 2015, **165**, 555.

[16] Y. Zhu, X. Kong, S. Zhu, F. Dong, H. Zheng, Y. Zhu and Y. Li, *Appl. Catal. B*, 2015, **166–167**, 551.

[17] D. Damodara, R. Arundhathi and P.R. Likhar, *Adv. Synth. Catal.*, 2014, **356**, 189.

[18] F. Santoro, R. Psaro, N. Ravasio and F. Zaccheria, *RSC Adv.*, 2014, **4**, 2596.

[19] K. Shimizu, K. Shimura, M. Nishimura and A. Satsuma, *RSC Adv.*, 2011, **1**, 1310.

[20] N.R. Kim, K. Shin, I. Jung, M. Shim and H.M. Lee, *J. Phys. Chem. C*, 2014, **118**, 26324.

[21] Z. Wang, P. Fongarland, G. Lu and N. Essayem, *J. Catal.*, 2014, **318**, 108.

[22] C. Xu, J. Sun, B. Zhao and Q. Liu, *Appl. Catal. B*, 2010, **99**, 111.

[23] J.M.L. Nieto, A. Dejoz and M.I. Vazquez, *Appl. Catal. A*, 1995, **132**, 41.

[24] Y.Z. Chen, C.M. Hwang and C.W. Liaw, *Appl. Catal. A*, 1998, **169**, 207.

[25] A. Villa, A. Gaiassi, I. Rossetti, C.L. Bianchi, K. Benthem, G.M. Veith and L. Prati, *J. Catal.*, 2010, **275**, 108.

[26] J.P. Espinós, J. Morales, A. Barranco, A. Caballero , J.P. Holgado and A.R. González-Elipe, *J. Phys. Chem. B*, 2002, **106**, 6921.

[27] Z. Chen, D. Mochizuki, M.M Maitani and Y. Wada, *Nanotechnology*, 2013, **24**, 265602.

[28] J. Czaplinska, I. Sobczak and M. Ziolek, *J. Phys. Chem. C*, 2014, **118**, 12796.

[29] K.D. Malviya and K. Chattopadhyay, *J. Phys. Chem. C*, 2014, **118**, 13228.

[30] H. Peng, W. Qi, S. Li and W. Ji, *J. Phys. Chem. C*, 2015, **119**, 2186.

[31] A. Cao, R. Lu and G. Veser, *Phys. Chem. Chem. Phys.*, 2010, **12**, 13499.

[32] Y. Wang, J. He, C. Liu, W. Chong and H. Chen, *Angew. Chem. Int. Ed.*, 2015, **54**, 2022.

[33] E.R. Sacia, M. Balakrishnan and A.T. Bell, *J. Catal.*, 2014, **313**, 70.

[34] J. Luo, J. Yu, R.J. Gorte, E. Mahmoud, D.G. Vlachos and M.A. Smith, *Catal. Sci. Technol.*, 2014, **4**, 3074.

[35] C. Xu, Y. Du, C. Li, J. Yang and G. Yang, *Appl. Catal. B*, 2015, 164, 334.

[36] T. Mitsudome, Y. Mikami, K. Ebata, T. Mizugaki, K. Jitsukawa and K. Kaneda, *Chem. Commun.*, 2008, 4804.

[37] T. Mitsudome, Y. Mikami, H. Funai, T. Mizugaki, K. Jitsukawa and K. Kaneda, *Angew. Chem.*, 2008, **120**, 144.

Table captions

Table 1 Nitrogen physisorption data of Cu-Ag catalysts

Table 2 Etherification of benzyl alcohol and 1-phenyl ethanol catalyzed by γ-Al_2O_3 [a]

Table 3 Dehydrogenation cross-coupling reaction of other primary and secondary alcohols

Table 4 Reusability of Cu-Ag/HT [a]

Figure captions

Fig. 1 Nitrogen physisorption isotherms (■, adsorption; ●, desorption) and Barrett–Joyner–Halenda (dV–dlogD) pore size distribution (inset) for Cu-Ag catalysts

Fig. 2 XRD patterns of HT supports and Cu-Ag/HT catalysts

Fig. 3 XRD patterns of MgO and γ-Al_2O_3 supports, and their supported Cu-Ag catalysts

Fig. 4 XRD patterns of 1 wt% Cu-Ag/HT and 10 wt% Cu-Ag/HT

Fig. 5 XPS spectra of Cu 2p and Ag 3d for 10 wt% Cu-Ag/HT

Fig. 6 Cu 2p XPS spectra of Cu 2p for catalysts stored for two or three months for (a) Cu-Ag/HT and (b) Cu/HT

Fig. 7 STEM images and SAED patterns of Cu-Ag/HT catalysts calcined and reduced at (a) 300 °C and (b) 600 °C. Inset: HR-TEM images of the

selected area.

Fig. 8 (A) CO_2-TPD and (B) NH_3-TPD profiles of supports: (a) HT, (b) MgO, and (c) γ-Al_2O_3.

Fig. 9 Effect of Mg:Al ratio on activity and selectivity of Cu-Ag catalysts. Reaction conditions: benzyl alcohol (1.0 mmol), 1-phenylethanol (1.0 mmol), catalyst (0.1 g), *o*-xylene (3 mL), 150 °C, 1 bar N_2, reaction time of 0.5 h.

Fig. 10 Effect of Cu:Ag mass ratio on catalytic activity of Cu-Ag/HT in the dehydrogenation cross-coupling reaction. Reaction conditions: benzyl alcohol (1.0 mmol), 1-phenylethanol (1.0 mmol), Cu-Ag/HT (0.1 g), *o*-xylene (3 mL), 150 °C, 1 bar N_2.

Fig. 11 Catalytic activity versus standing time for (a) Cu-Ag/HT and (b) Cu/HT catalysts. Reaction conditions: primary alcohol (1.0 mmol), secondary alcohol (1.0 mmol), *o*-xylene (3mL), catalyst (0.1 g), 150 °C, 1 bar N_2, reaction time of 1 h.

Table 1 Nitrogen physisorption data of Cu-Ag catalysts

Entry	Samples	Metal ratio (Mg:Al)[a]	Surface area (m^2g^{-1})[b]	Pore volume (cm^3g^{-1})[c]	Pore diameter (Å)
		Prepared/determined			
1	Cu-Ag/γ-Al_2O_3	0:1/0:1	200	0.58	78
2	Cu-Ag/HT	1:1/1.25:1	229	1.12	127
3	Cu-Ag/HT	2:1/2.08:1	198	0.60	102
4	Cu-Ag/HT	3:1/2.96:1	209	0.66	96
5	Cu-Ag/HT	5:1/5.63:1	202	0.49	73
6	Cu-Ag/MgO	1:0/1:0	125	0.44	105

[a] Determined by energy-dispersive X-ray spectroscopy. [b] Calculated by the BET method. [c] Calculated by the Barrett–Joyner–Halenda method from the desorption isotherm.

Table 2 Etherification of benzyl alcohol and1-phenyl ethanol catalyzed by γ-Al_2O_3[a]

Entry	Reaction time	Conversion of benzyl alcohol (%)	Yields (%)		
			Dibenzyl ether	1-methyl benzyl ether	1,1′-diphenyl ether
1	45 min	81	0.2	49	2.9
2	1 h	87	0.4	58	3.6
3	1.5 h	88	0.3	69	4.0
4	2 h	99	0.5	95	2.6

[a] Reaction conditions: benzyl alcohol (1.0 mmol), 1-phenylethanol, (1.0 mmol), catalyst (0.1 g), o-xylene (3 mL), 150 °C, 1 bar N_2.

Table 3 Dehydrogenation cross-coupling reaction of other primary and secondary alcohol

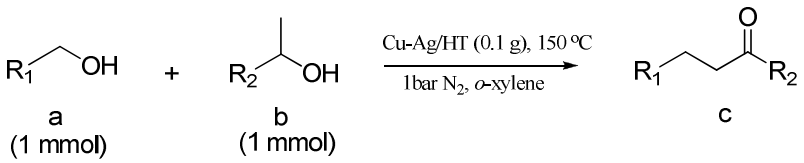

Entry	a	b	c	Reaction time (h)	Conversion of a (%)	Yield to c (%) [a]
1	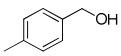		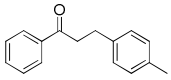	2	100	100
2	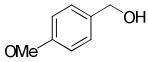		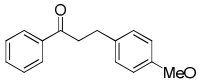	3	100	98
3	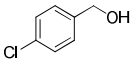		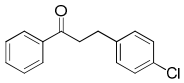	8	100	100
4	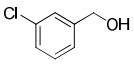		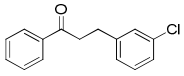	8	92	90
5	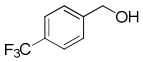		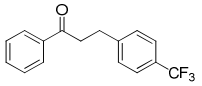	8	100	93
6	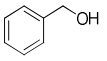	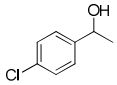	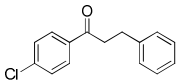	12	100	99
7	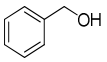	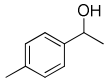	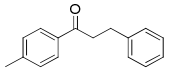	8	100	97
8	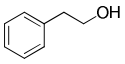		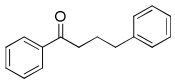	8	100	100
9	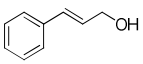		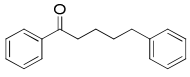	8	80	58
10	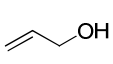		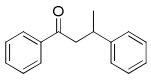	8	85	46
11	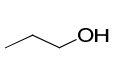		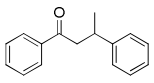	8	93	39

[a] Conversion and yield based on alcohol consumption.

Table 4 The reusability of Cu-Ag/HT catalyst [a]

Entry	Used times	Conversion of benzyl alcohol (%)	Yield to β-phenylpropiophenone (%)
1	1st	98	98
2	2nd	98	98
3	3rd	98	98
4	4th	98	95
5	5th	93	90
6	6th	85	80
7	7th	78	57
8	8th	55	24
9	9th	56	0.8

[a] The spent catalyst was washed with *o*-xylene three times, and then applied to the further run without any other treatment. Reaction conditions: primary alcohol (1.0 mmol), secondary alcohol (1.0 mmol), *o*-xylene (3 mL), Cu-Ag/HT (0.1 g), 150 °C, 1 bar N_2, 1 h.

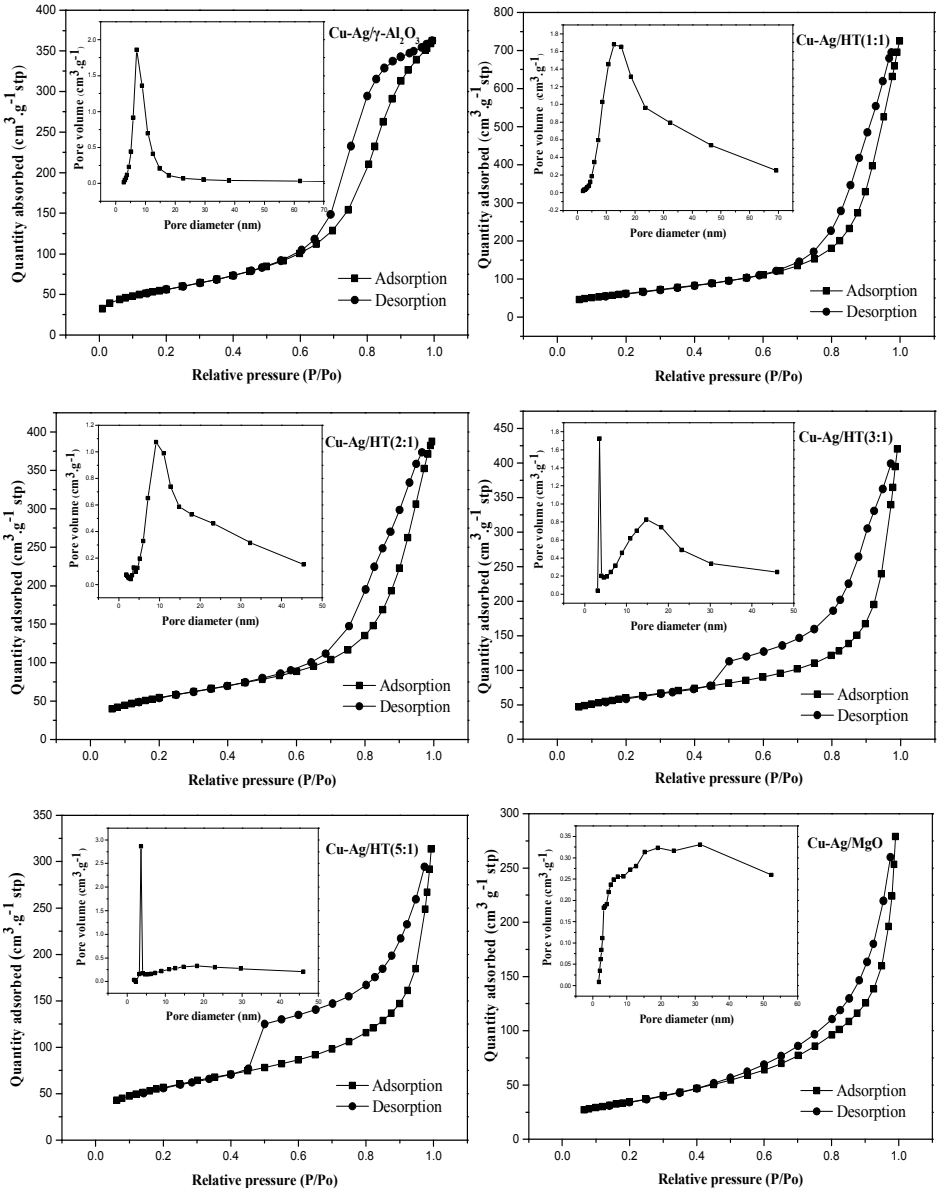

Fig. 1

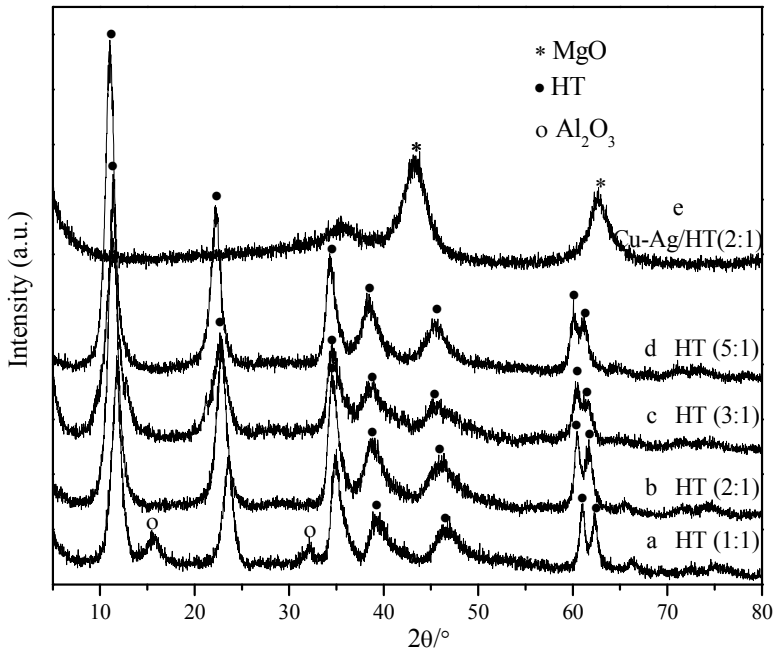

Fig. 2

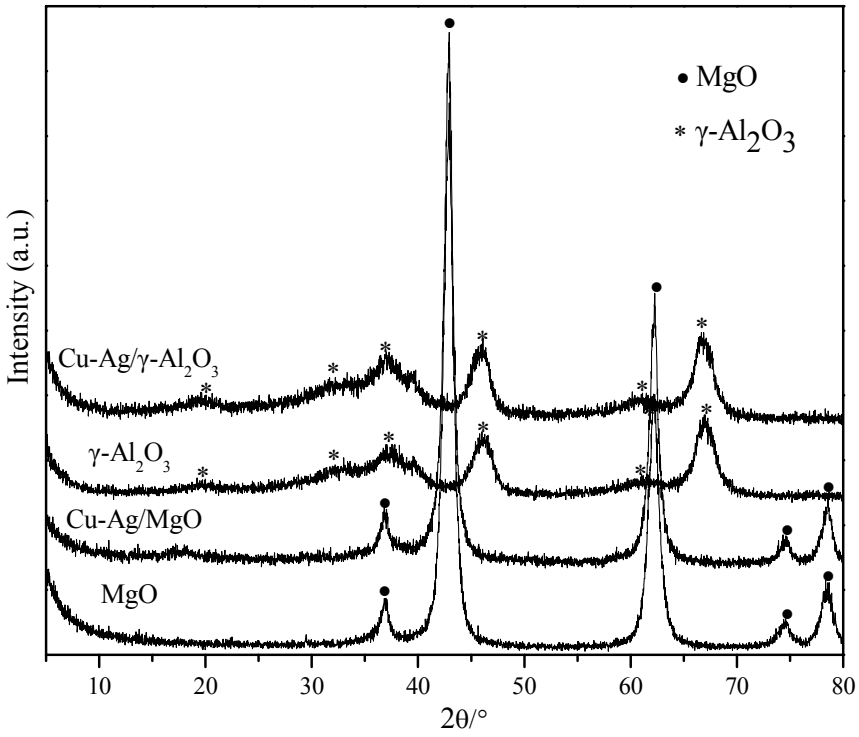

Fig. 3

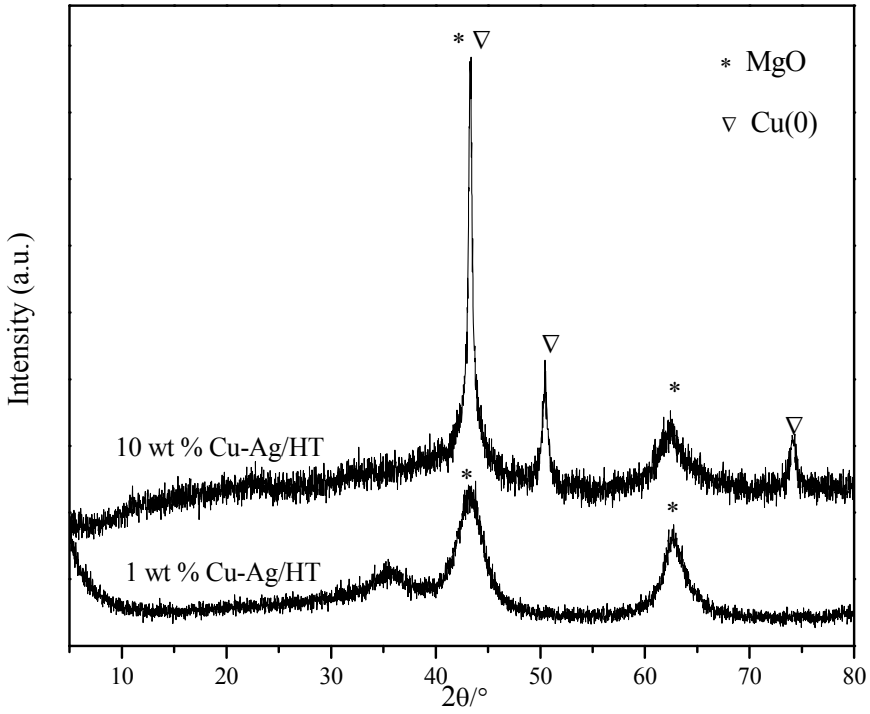

Fig. 4

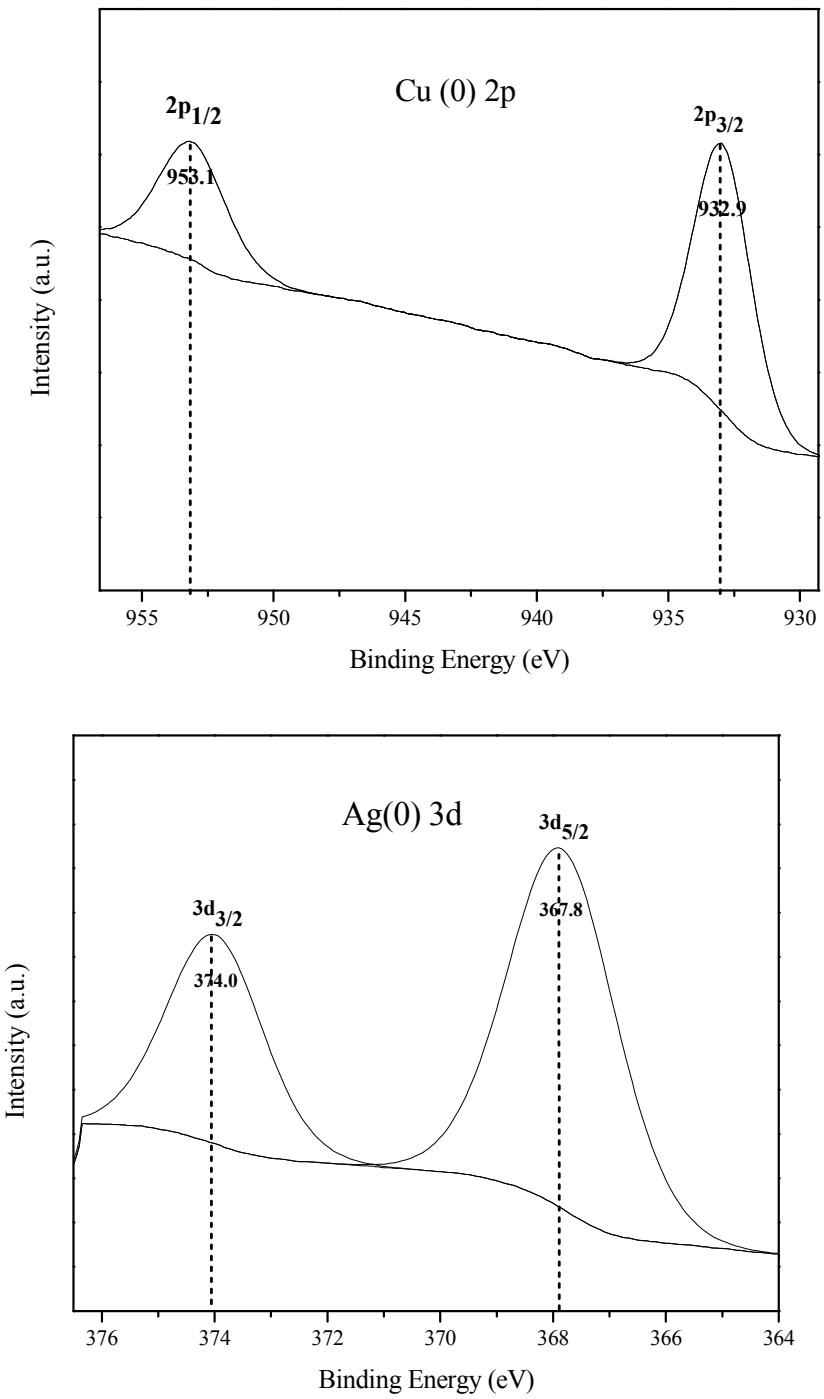

Fig. 5

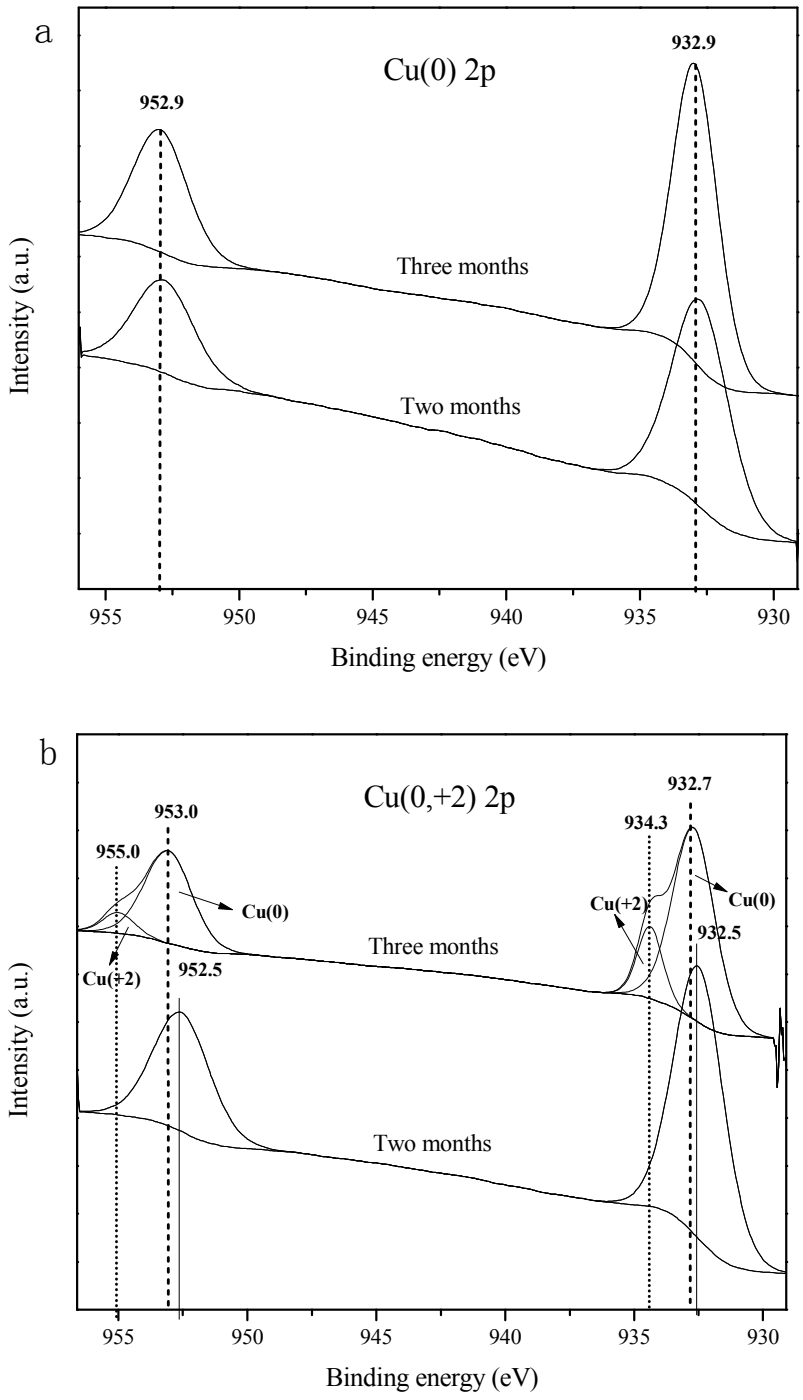

Fig. 6

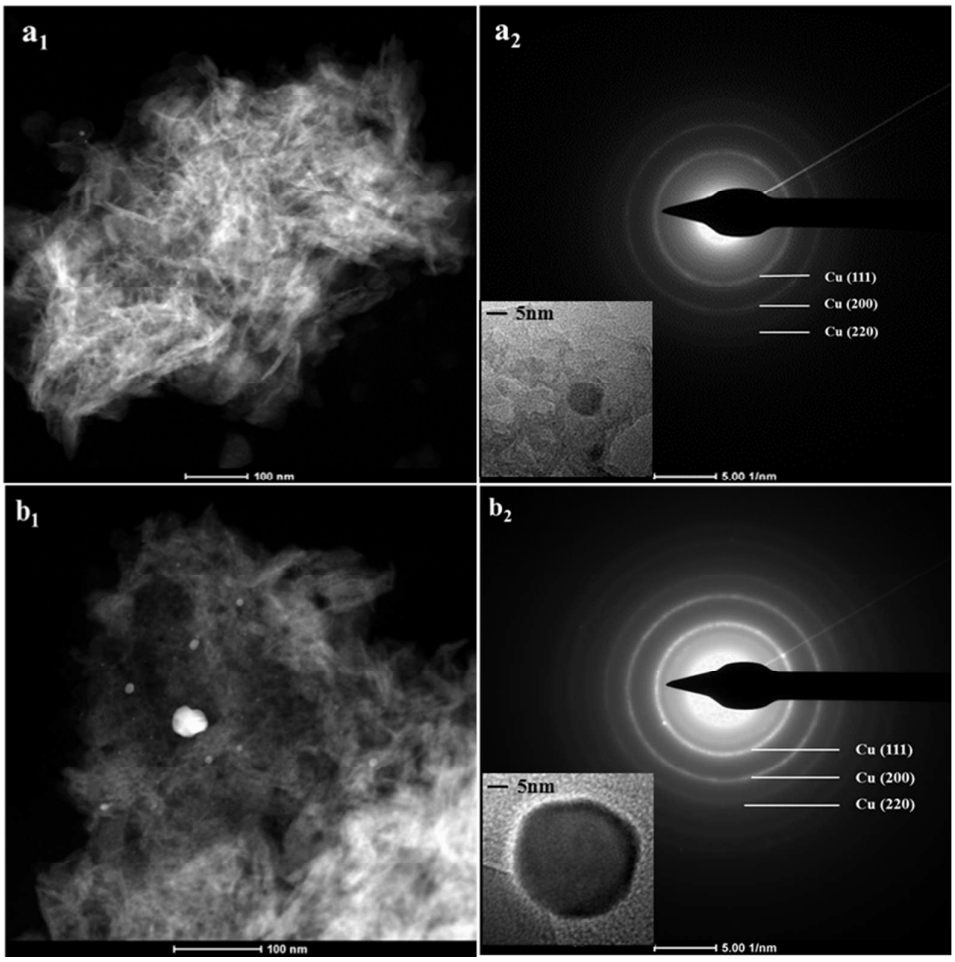

Fig. 7

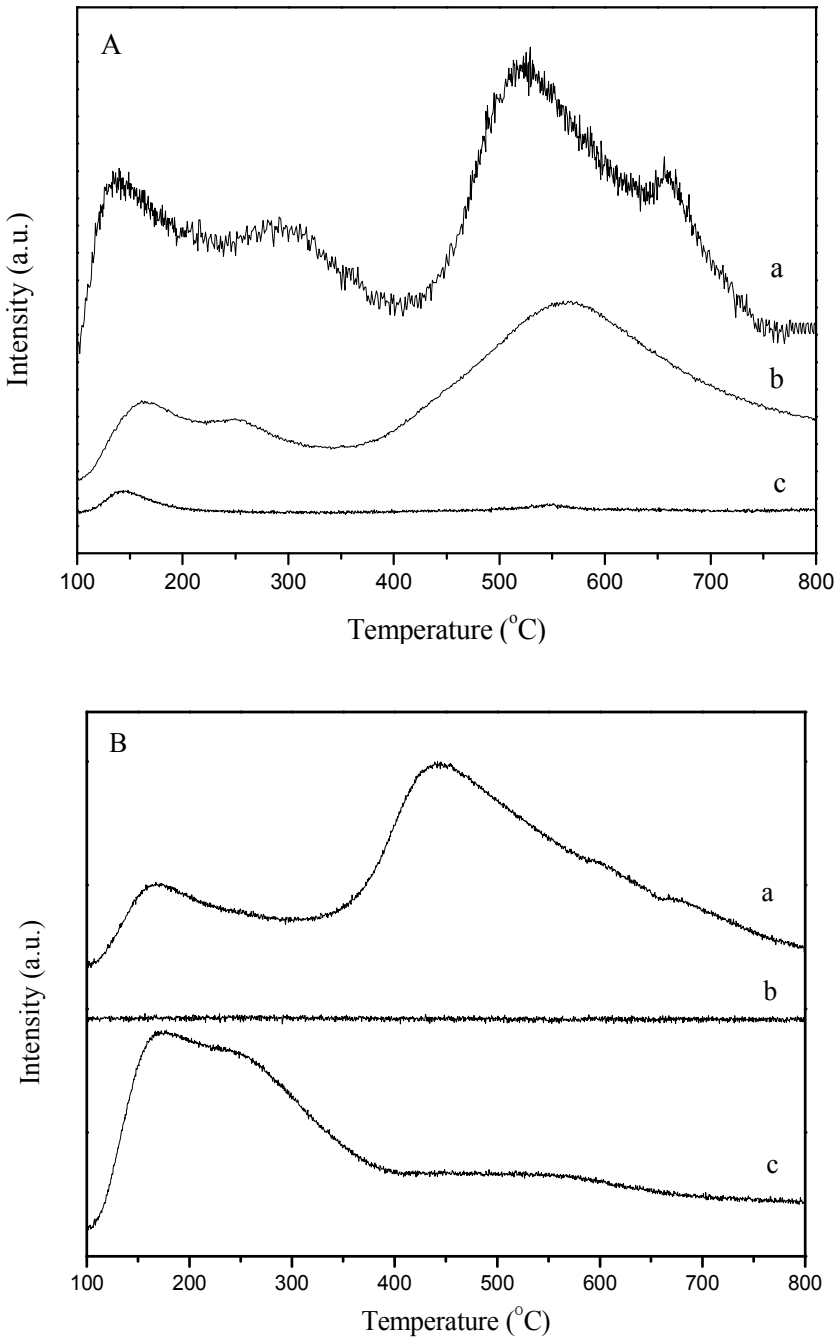

Fig. 8

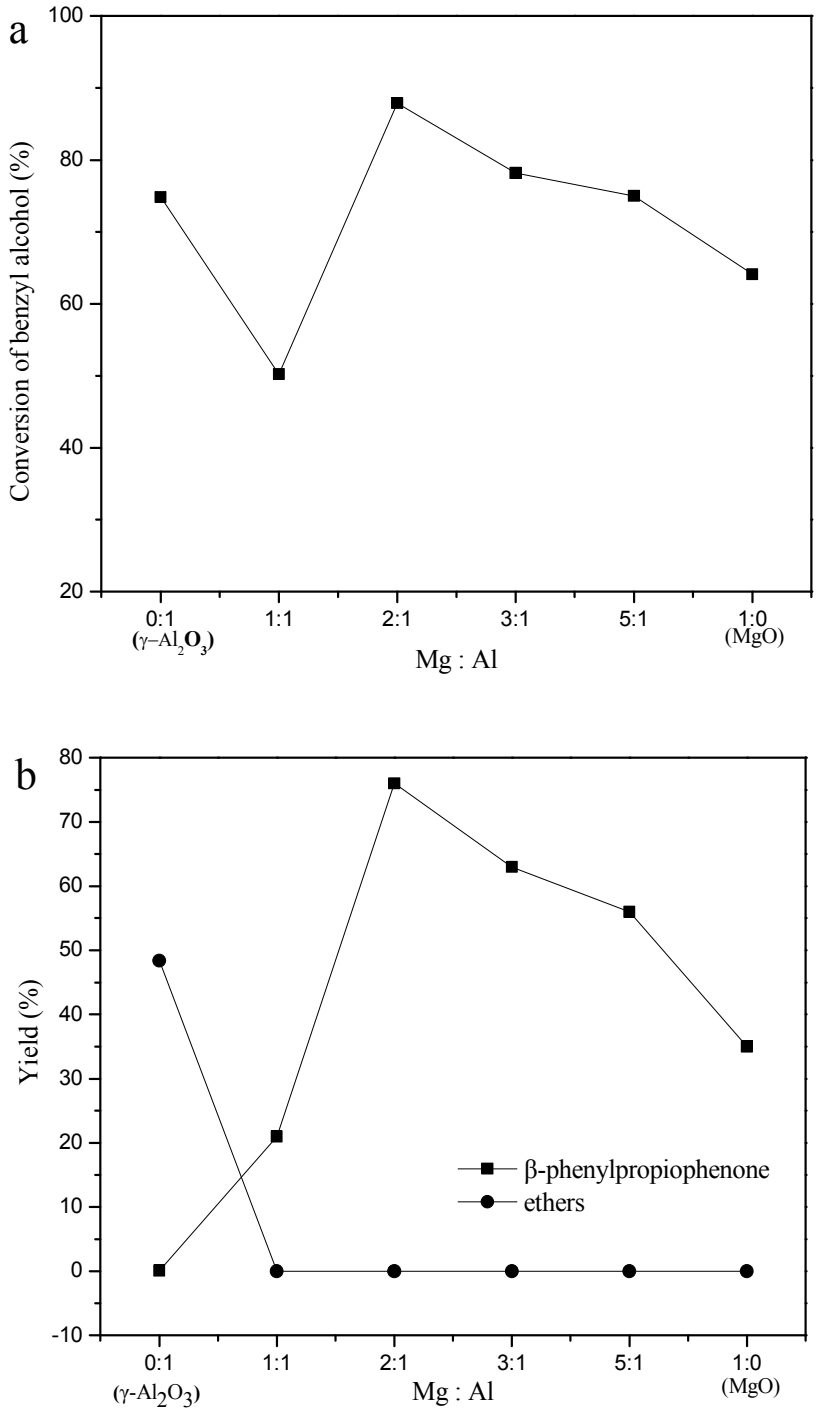

Fig. 9

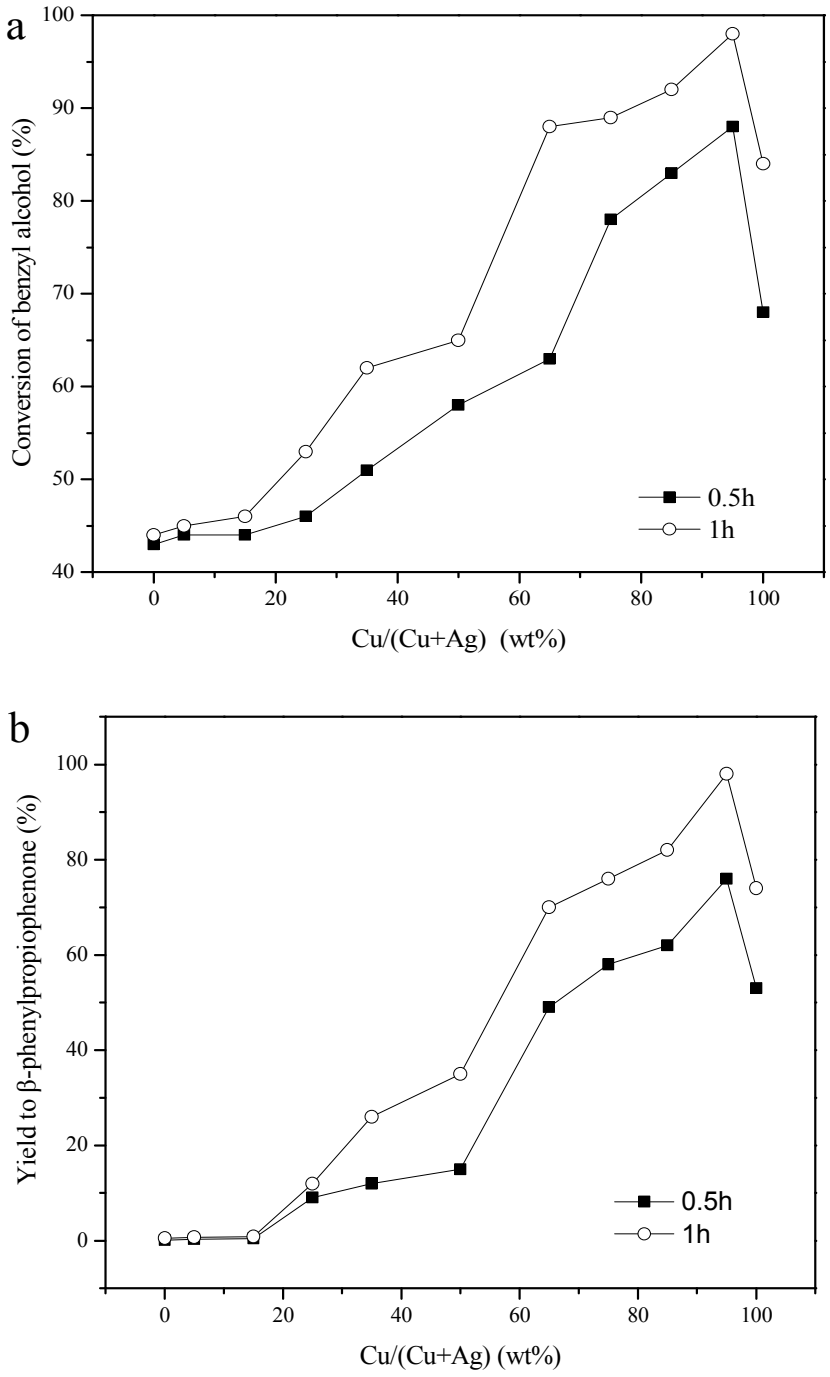

Fig. 10

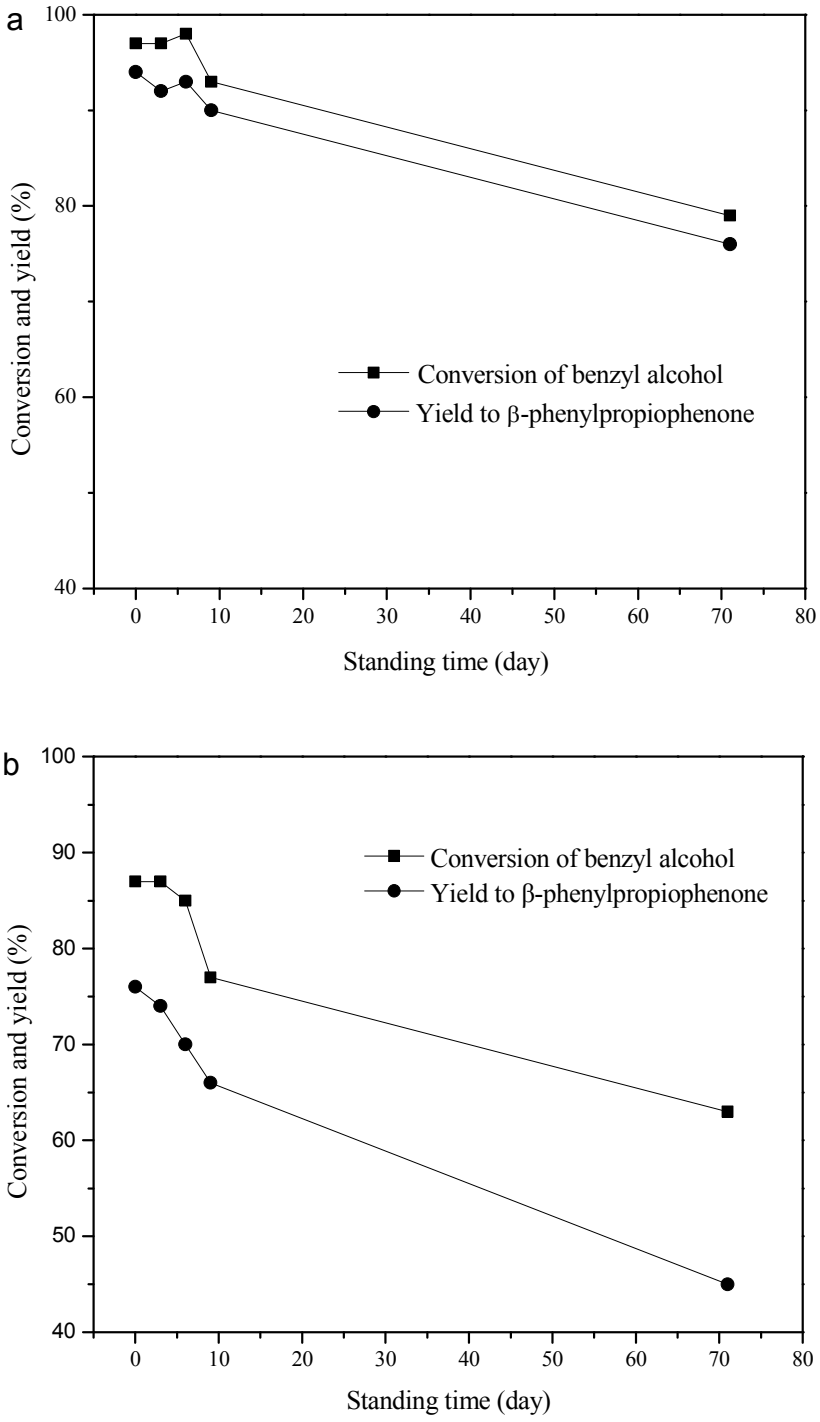

Fig. 11

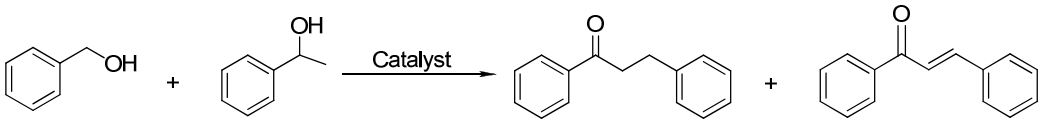

Scheme 1 Cross-coupling of primary and secondary benzylic alcohols.

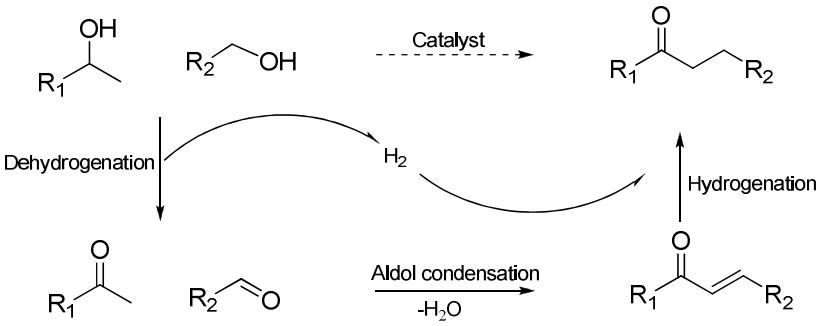

Scheme 2 Mechanism for the cross-coupling of primary and secondary alcohols to produce higher ketones.

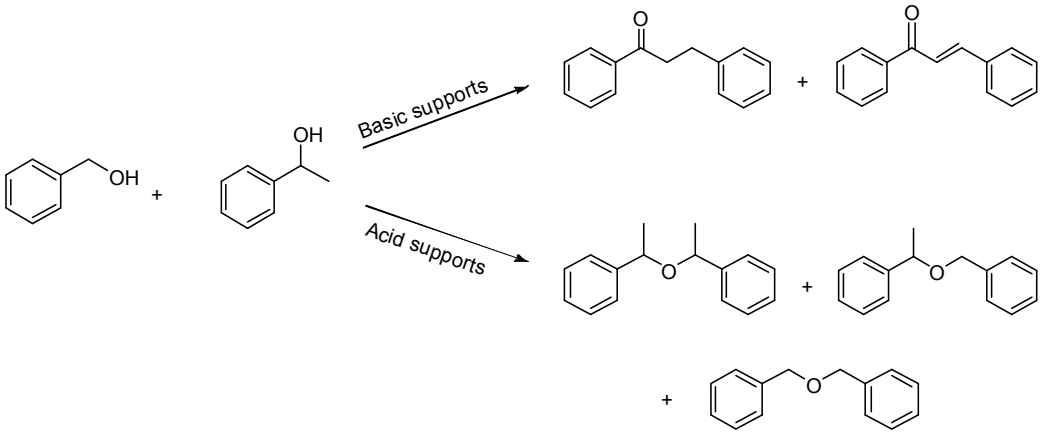

Scheme 3 Dehydrogenative cross-coupling or direct etherification of primary and secondary benzylic alcohols

Graphical abstract